Research Article

WIND ENGINEERING

Wind Engineering
1–21
© The Author(s) 2017
Reprints and permissions:
sagepub.co.uk/journalsPermissions.nav
DOI: 10.1177/0309524X17737052
journals.sagepub.com/home/wie
SAGE

A new modeling technique based on performance data for photovoltaic modules and horizontal axis wind turbines

Mohamed A Sharaf Eldean[1], Adel El Shahat[2] and AM Soliman[1,3]

Abstract

This article proposes new methods of modeling and simulation of photovoltaic and horizontal wind turbine systems. The photovoltaic and horizontal wind turbines are modeled by the use of actual data sheets listed in the lookup table model. Moreover, artificial neural network numerical technique is used to simulate and evaluate the designed systems. The implemented work may help the designer and investor to elect a specified photovoltaic module and/or the horizontal wind turbine according to the demanded power load, thence predicting the operating conditions before the establishment process. The results show good matching with the actual data for the photovoltaic and horizontal wind turbine systems.

Keywords

Photovoltaic, artificial neural networks, wind turbines, modeling and simulation, MATLAB–Simulink

Introduction

The renewable energy sources, such as solar, wind, tidal, geothermal, and so on, are attracting immense attention as an alternative energy. Among the renewable energy sources, the photovoltaic (PV) has been widely employed in low-power applications. Recently, PV array system is recognized and widely considered in electric power generation applications. PV module represents the fundamental power conversion unit of a PV generator system. During the design process of PV powered systems, a simulation must be performed for system analysis and parameter settings; therefore, an efficient and user-friendly simulation model of the PV is always needed. The state-of-the art of PV and/or wind turbine simulation are based on classical performance model, using parameters such as cell performance, temperature distribution, cell physical size, and so on, assuming the design and physical parameters. Unique to this article is how to build a simulation model based design technique of modeling, where the modeling generates design parameters related to performance. Taking PV as an example, the developed models are built based on *design* technique aspects of modeling but not *performance* technique. In performance model, areas current, voltage, and design limits are assigned (existing system) to calculate and measure the power, efficiency, and performance. However, in the design model (current case study), the PV power is assigned and known to calculate and measure the design limits such as, areas, diameters, current, voltage, module efficiency, required costs, and so on. In case of horizontal wind turbine (HWT), design parameters, such as hub height, rotor diameter, rotor speed, and so on, are left unspecified and become unknown based on the assigned power. For PV case, cell characteristics modeling example were implemented for that purpose in Burgelman et al. (2004), Kurtz et al. (2011), Zouari and Arab (2011), Chenni et al. (2007), Badescu (2006), and Kim et al. (2011). The performance issues of the PV based on the *I-V* relation were presented

[1]Department of Engineering Science, Faculty of Petroleum and Mining Engineering, Suez University, Suez, Egypt
[2]Electrical Engineering Department, Georgia Southern University, Statesboro, GA, USA
[3]Mechanical Engineering Department, Faculty of Engineering, Al Jouf University, Sakakah, Saudi Arabia

Corresponding author:
Mohamed A Sharaf Eldean, Department of Engineering Science, Faculty of Petroleum and Mining Engineering, Suez University, Suez 43722, Egypt.
Email: mwahab31@yahoo.com

according to Lo Brano et al. (2010), De Soto et al. (2006), Sandrolini et al. (2010), and Villalva et al. (2009). Example of field analysis, sizing, and applications of the PV were presented in Vazquez and Rey-Stolle (2008), Parida et al. (2011), Ghoneim et al. (2002), Ahmad and Schmid (2002), Abidin Firatoglu and Yesilata (2004), Hasnain and Alajlan (1998), and Ismail et al. (2013). The applications focused on the pumping water, desalination, lighting homes and streets, and some stations to generate electricity; however, the capacity does not exceed over 10 MW. Other in literature focus on the optimization-based genetic algorithm or neural network simulation tool boxes (Ammar et al., 2013; Ashhab, 2008; Mellit and Pavan, 2010; Zhang and Bai, 2005). Such techniques of optimization dealt with the PV matter as a cell, module, or a small system. The common factor between the past works is that their developed models addressed a performance matter not a design matter. Based on the same approach, wind turbines have proven their viability, solving the mathematical models representing HWT units which are tedious and repetitive problem (Nafey et al., 2010). Nested iterative procedures are commonly required to solve these models. Likewise, the process configurations are characterized by the existence of a number of recycled streams. To tackle the mathematical problems (forward and backward streams), several researchers have developed different methods, techniques, and computer programs for the simulation of a very wide range of variety of wind turbines (http://www.awsopenwind.org/; http://www.windsim.com/product-overview.aspx; Bououden et al., 2012; Emami and Noghreh, 2010; Hansen et al., 2006; Janajreh et al., 2010; Jafarian and Ranjbar, 2010; Kusiak and Song, 2010; Thapar et al., 2011). The previous work on the modeling of wind turbines is almost focused on some following pin points:

- Utilization of fuzzy and neural toolboxes to measure and evaluate the performance of the existing turbines.
- Most of these examples are performed at low orbit of power demand. Also, they addressed a specific case and were enforced by the use of momentum and mass continuity equations.
- Most of these models are not simple enough to be implemented by investors or ordinary engineers.
- It requires a previous knowledge of the environment or the operating conditions.
- Most of the literature models are constructed based on complicated differential equations.

It is obvious from the literature for both PV and HWT systems that the most of such mathematical models were performed based on the performance technique and not applied to the design technique. Moreover; it was built for special cases and not for a wide range of operating conditions. Concurrently, the developed power and power coefficient are unknown or even specified. The review confirmed that there is a pressing case to develop a new code with some specific features such as simplicity, generality, and easy to deal with. In this work, a new graphical user interface (GUI) model for simulating of the PV and HWT is presented. Moreover, artificial neural network (ANN) algorithm is used to simulate the PV and HWT to compare the results with the test data fitness from the manufacture manuals. This modular model code has great capabilities to overcome previous programming problems and limitations such as the recycle streams and differential equations problems. The remarkable simplicity shows that the developed code may help the user or the designer to pick out a suitable PV and/or HWT units based on only the power demanded (one parameter) by specifying the load. Thus, user has no need for extensive knowledge of the complicated equations or correlations of the aerodynamics or solar beams characteristics. Furthermore, the new code has a very good accuracy results that been matched well with the actual data sheet that has been recorded by the manufacture manual.

The process modeling techniques

Engineering processes consist of a number of interactive units. Using these units in a wide range of process, configurations and types can be obtained. Generally, to understand the behavior of these processes under different operating conditions, a flexible and general computer program is really needed. Using such program, a large number of flow sheeting problems can be controlled. These problems can be broadly divided into two classes: (a) *performance problems* and (b) *design problems* (current model). In the performance problem, the variables associated with the feed streams to a process unit and all design parameters (such as PV module area, and PV panel's dimensions) are assumed to be known. The variables associated with the internal and output streams are the unknowns. In the design problem, unique to this work, some design parameters (areas, dimensions, voltage, current, number of cells, unit cost, etc.) and/or feed variables are left unspecified and become unknown to be determined. What is left known in general is the boarder streams of the process or the system and in such case, is the superpower of the PV module. To simulate and predict the characteristics of different types of PV system, a lot of real data are taken from a real manufacture manual of each module type. It is projected that by identifying the output power from the system application, the design limits would be counted. The PV system is modeled according to the actual data presented through more than 3150 data points from the manufacturing manuals. MATLAB–SimuLink (http://www.mathworks.com/index.html) browser is used to model and visualize the PV and/or HWT system program. The design limits for the PV example are summarized as follows:

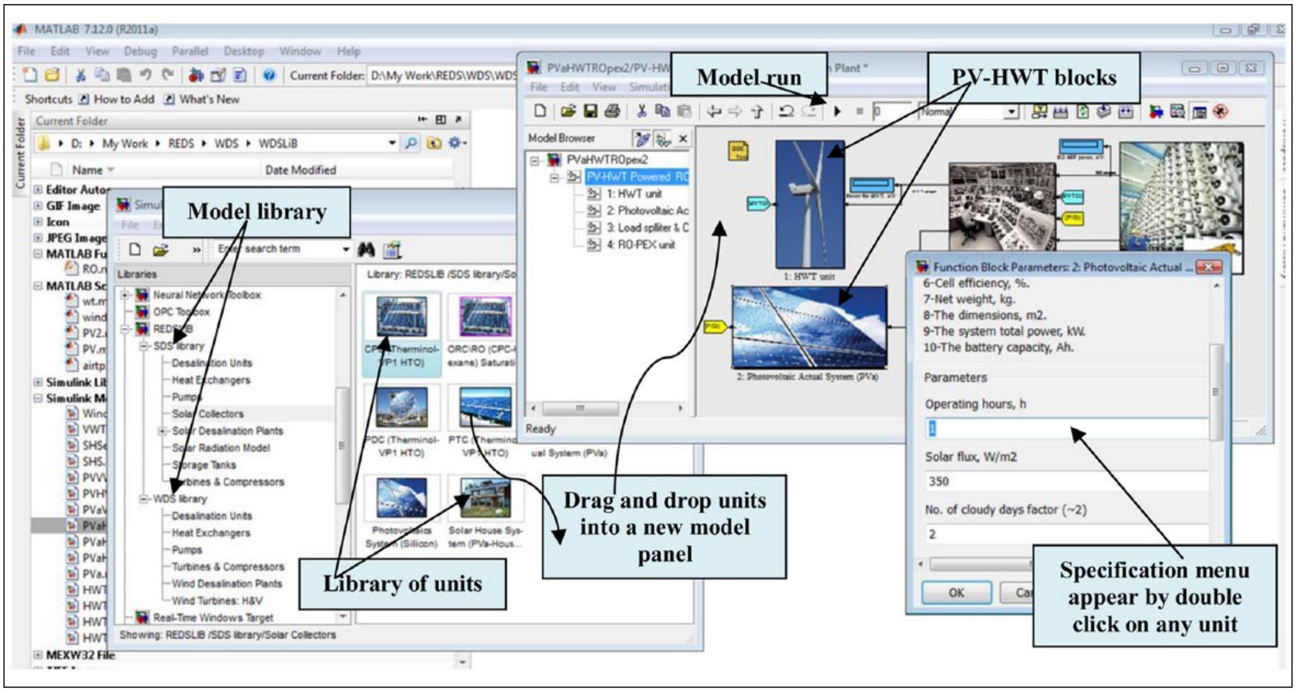

Figure 1. Photograph of the developed code for both PV and HWT.

- The open circuit voltage V and the short circuit current A;
- The maximum voltage and current;
- The cell and module efficiencies;
- The number of cells and modules of the system;
- The module and system weights, dimensions, and areas;
- The battery bank capacity;
- The total costs of the system.

Regarding to HWT, a lot of real data are taken from the manufacture manual of each case. It is proposed that by identifying the output power from the turbine unit, the design limits would be calculated. The design limits are summarized as follows:

- Starting wind speed (m/s);
- Average wind speed (m/s);
- Hub height (m);
- Rotor diameter (m);
- The rotor speed (RPM);
- The unit cost ($);
- Number of blades in case of vertical type.

MATLAB tool box (http://www.mathworks.com/index.html) is used to predict the characteristics correlations based on a non-linear and ANN techniques. In the following subsections, the uses of MATLAB tool box help the author to construct the new model library by the aid of the GUI. The constructed modules are built using the lookup-table correlation method and the ANN tool box. Figure 1 shows the photograph of the software library that represents the PV and/or HWT models. User can easily drag and drop the module or the unit from the side library to construct the system.

The new modeling techniques of the PV

The PV model that is presented in this work is completely differing from any other presented models in the literature. The main differences concluded in that the actual data presented in the core code of the model are performing the code itself. Data manuals are fed into the core of the code to give a real sense of the curve fitting. Two methods are used in this study;

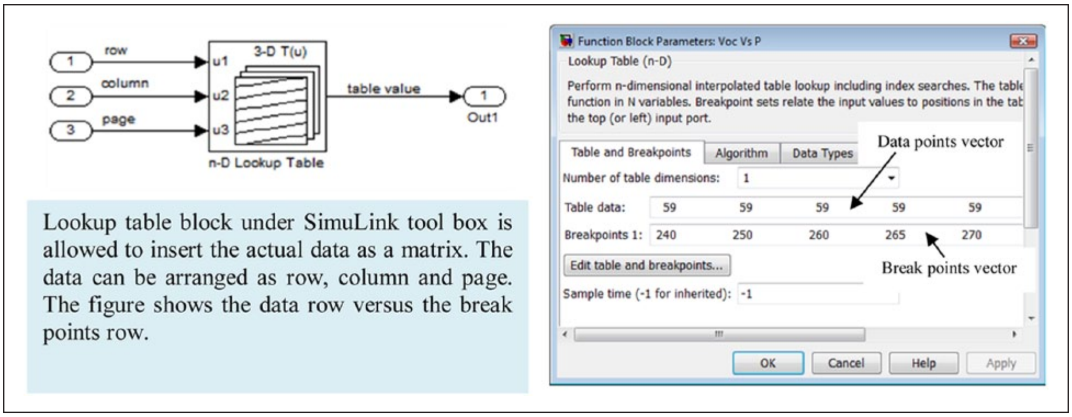

Figure 2. Schematic diagram of the n-D lookup table.

the first is the use of polynomial lookup tables of Simulink tool box (polynomial interpolation), whereas the second is the use of ANN tool box under the same tool box.

Lookup table method for PV

The n-D lookup table block evaluates a sampled representation of a function in N variables $y = F(x_1, x_2, x_3, \ldots, x_n)$ where the function F can be empirical. The block maps inputs to an output value by looking up or interpolating a table of values you define with block parameters. The block supports flat (constant), linear, and cubic-spline interpolation methods. In case of matching the values of indices in breakpoint data sets, it outputs the table value at the intersection of the row, column, and higher dimension breakpoints. The main advantage of such method is that user can easily specify one or two parameters to obtain many parameters. Only the user has to feed the lookup table with the accurate and required data from the manual.

In case of no matching of the values of indices in breakpoint data sets, but if within range, then interpolates appropriate table values, using the interpolation method of use choice. In case nonmatching data are out of range, extrapolates the output value, use the extrapolation method. In this study, the range of the operating module type is from 5 to 280 W. Each module watt type can calculate the module specification based on the data fed in the table. Figure 2 shows the schematic diagram of the lookup table polynomial method.

Based on the module power, the following code can be calculated. The number of PV modules (NOM) could be calculated based on total power and module power

$$NOM = \frac{P_t}{P_m} \tag{1}$$

And the module area (m^2) is then calculated

$$A_m = 100 \times \frac{P_m}{G_b \times \eta_m} \tag{2}$$

Then the total area (m^2) can be calculated

$$A_t = A_m \times NOM \tag{3}$$

The cell area (cm^2) based on the number of cells (NC) has been calculated from the lookup table

$$A_c = \frac{A_m \times 10^3}{NC} \tag{4}$$

The battery storage (WH) based on the operating hours (OH), number of cells (NC), the total power (P_t), battery efficiency, and depth of discharge (DOD) is calculated as follows

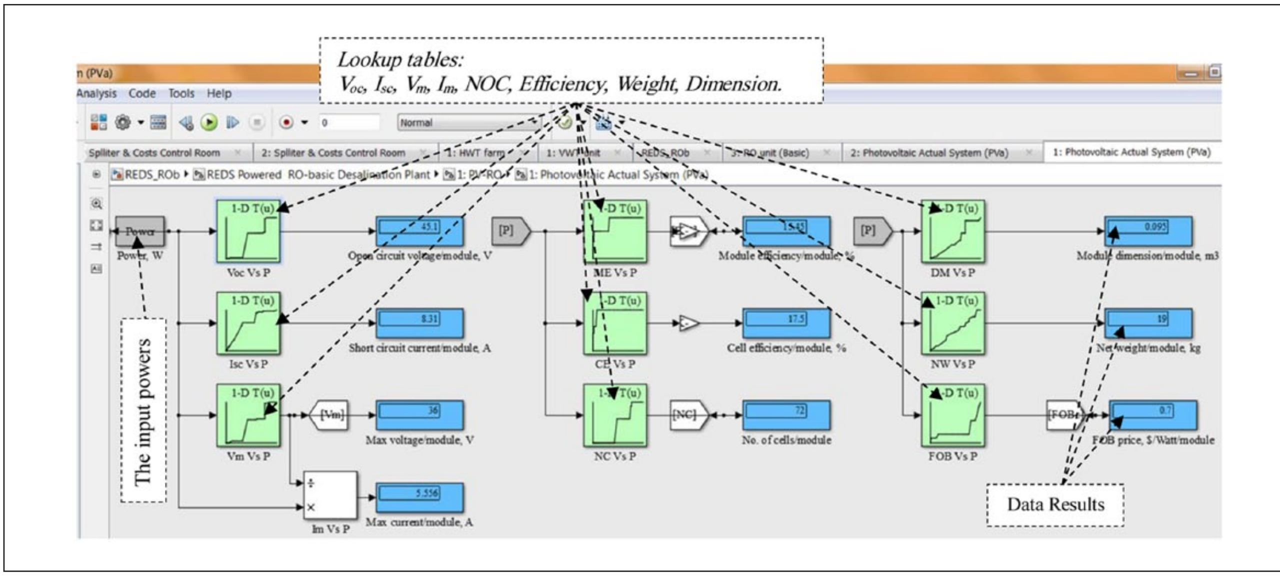

Figure 3. Lookup tables results for PV model browser.

$$BS = \frac{OH \times NOC \times P_t}{DOD \times \eta_b} \tag{5}$$

If a 24-V system is chosen, then the required AH of batteries = 16,585/24,700 AH

$$AH = \frac{BS}{V_m} \tag{6}$$

Number of batteries can be calculated as follows based on the maximum voltage and the battery voltage

$$NOB = \frac{V_m}{V_b} \tag{7}$$

The system total costs in (C_t, $) are then calculated based on the full over board costs of the modules (FOB_c) and the battery costs (C_b)

$$C_t = (P_t \times FOB_c) + (C_b \times NOB) \tag{8}$$

where the FOB_c includes the cables, connections, workers' time, inverter unit, and the maintenance costs. Figure 3 shows the model browser of the PV under the construction of polynomial look up table method. The presented model associated with the above method has some important features, eliminating the need for user to deal with complicated code or equations, such as the following:

- *Easy model handling*. It can be easily built by the use of the lookup table block where the hard part is to collect and arrange the needed data vector.
- The main specifications are easily calculated based on one parameter (the identification of the module power can drive out nine parameters). However, in the other modeling techniques, it is not found that one parameter can result out in nine parameters.
- Such technique of modeling is not investigated before.

ANN method for PV

An ANN consists of very simple and highly interconnected processors called neurons. The neurons are connected to each other by weighted links over which signals can pass. Each neuron receives multiple inputs from other neurons

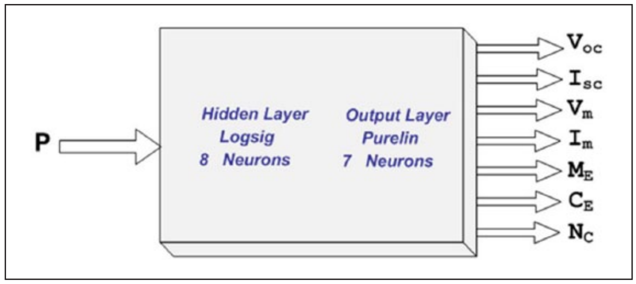

Figure 4. Schematic diagram of PV ANN model.

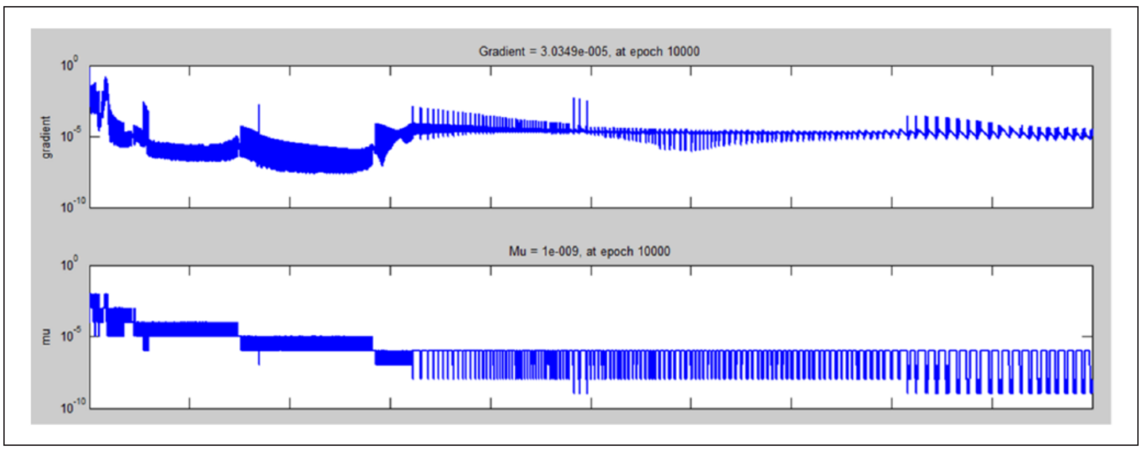

Figure 5. The training results for the proposed PV ANN model.

in proportion to their connection weights and generates a single output which may propagate to several other neurons. Among the diverse kinds of ANNs that exist, the back-propagation learning algorithm has become the most popular used method in engineering application. To develop the PV code model, recurrent neural network model is employed. The number of time-delays to be employed in the proposed network is determined by performing a cross-correlation analysis. The cross-correlation analysis can be used to observe the interaction strength between two signals. The analysis can also be used to detect whether a time lag exists between the signals. It has been shown in the literature that time-delay estimation between two continuous signals can be done by detecting peaks in the cross-correlation function. In this study, a cross-correlation analysis is performed to determine the interaction force between the input variables and outputs. The Levenberg–Marquardt back-propagation algorithm is utilized for training, which is performed in the neural network toolbox of MATLAB. For the design of PV system, commercial PV modules are generally considered to be built in the PV power plants. So, this part presents a simple but efficient PV modeling trial for both specific and general one. The result shows that the PV model using the equivalent circuit in moderate complexity provides better matching with the real PV module. Figures 4 and 5 show the schematic diagram of the PV under ANN tool box and the training results, respectively. Figure 4 shows that one input (power) with hidden layer of eight neurons would result in seven outputs based on seven neurons for the output layer. This would result in a best fitness based on training iterations as presented in Figure 5. The advantage of this ANN model is that one input (power) can generate and predict the all output parameters. This operation is quite impossible for the other literature models.

The ANN generated code is developed based on the following equations. The normalized power Pn in equation (9) presents the normalized input for the power and the following equations lead to the required derived equation, where n subscript denotes normalized parameters, Ei is the sum of input with input weight and input bias for each node in a hidden layer in a neural network, Fi is the output from each node in a hidden layer to output layer according to transfer function and here is log-sig

$$Pn = \frac{P_m - 154.1228}{86.9785} \tag{9}$$

$$E1 = -324.6058 \times Pn + 430.2332 \tag{10}$$

$$F1 = \frac{1}{1 + exp^{-E1}} \tag{11}$$

$$E2 = 292.1159 \times Pn - 307.4633 \tag{12}$$

$$F2 = \frac{1}{1 + exp^{-E2}} \tag{13}$$

$$E3 = 47.5094 \times Pn - 35.5277 \tag{14}$$

$$F3 = \frac{1}{1 + exp^{-E3}} \tag{15}$$

$$E4 = 1.8250 \times Pn + 1.7837 \tag{16}$$

$$F4 = \frac{1}{1 + exp^{-E4}} \tag{17}$$

$$E5 = 142.7159 \times Pn + 75.2497 \tag{18}$$

$$F5 = \frac{1}{1 + exp^{-E5}} \tag{19}$$

$$E6 = -55.6915 \times Pn - 89.3902 \tag{20}$$

$$F6 = \frac{1}{1 + exp^{-E6}} \tag{21}$$

$$E7 = 131.8635 \times Pn + 176.6258 \tag{22}$$

$$F7 = \frac{1}{1 + exp^{-E7}} \tag{23}$$

$$E8 = -56.1527 \times Pn - 90.14 \tag{24}$$

$$F8 = \frac{1}{1 + exp^{-E8}} \tag{25}$$

The following are the normalized outputs relations from ANN:

The normalized open circuit voltage is obtained as follows

$$\begin{aligned} V_{OCn} &= 0.2603 \times F1 - 0.8646 \times F2 + 1.5262 \times F3 - 0.7479 \times F4 + 1.6856 \times F5 - 27.716 \times F6 \\ &\quad + 0.1945 F7 + 27.5989 \times F8 - 1.2466 \end{aligned} \tag{26}$$

Table 1. The unnormalized correlations for the desired output parameters.

Output parameter	Correlation
Open circuit voltage	$V_{OC} = 11.0323 \times V_{OCn} + 35.0009$
Short circuit current	$I_{SC} = 2.785 \times I_{SCn} + 5.4497$
Maximum voltage	$V_m = 9.3979 \times V_{mn} + 27.2772$
Maximum current	$I_m = 2.6309 \times I_{mn} + 5.0547$
Module efficiency	$\eta_m = 0.0059 \times \eta_{mn} + 0.1350$
Cell efficiency	$\eta_c = 0.0116C \times \eta_{cn} + 0.1675$
Number of cells	$NOC = 18.9866 \times NOC_n + 58.7895$

The normalized short circuit current is obtained as follows

$$I_{SCn} = -0.3577 \times F1 + 0.4036 \times F2 - 0.6836 \times F3 + 6.0477 \times F4 - 1.4217 \times F5 \\ + 29.7807 \times F6 - 0.4409 \times F7 - 29.7082 \times F8 - 2.7748 \tag{27}$$

The normalized maximum current and voltage are obtained as follows

$$V_{mn} = 1.6336 \times F1 - 0.9422 \times F2 + 1.577 \times F3 - 0.5747 \times F4 + 1.4615 \times F5 - 33.4875 \times F6 \\ + 0.1497F7 + 33.352 \times F8 - 2.484 \tag{28}$$

$$I_{mn} = -0.4981 \times F1 + 0.4071 \times F2 - 0.6475 \times F3 + 5.4252 \times F4 - 1.1416 \times F5 + 9.683 \times F6 \\ - 0.3647F7 - 9.6696 \times F8 - 2.4307 \tag{29}$$

The normalized efficiencies of the module and the cell are obtained, respectively, as follows

$$\eta_{mn} = 0.0193 \times F1 - 0.5307 \times F2 + 0.1383 \times F3 + 1.2274 \times F4 - 1.5651 \times F5 - 963.6758 \times F6 \\ + 0.6763 \times F7 + 962.8663 \times F8 - 0.104 \tag{30}$$

$$\eta_{cn} = -0.0523 \times F1 + 0.1946 \times F2 - 0.4488 \times F3 + 3.5823 \times F4 - 0.6633 \times F5 - 945.6335 \\ \times F6 - 1.7534 \times F7 + 943.8266 \times F8 - 0.4238 \tag{31}$$

The normalized number of cell parameter is obtained as follows

$$NOC_n = 0.0194 \times F1 - 1.2485 \times F2 + 1.6434 \times F3 + 3.1176 \times F4 + 0.1489 \times F5 - 64.457 \\ \times F6 - 0.8867 \times F7 + 64.9028 \times F8 - 2.0399 \tag{32}$$

The un-normalized output relations are listed in Table 1.

The new modeling techniques of the HWT

Lookup table method for HWT

The wind turbine model is designed and simulated via the same platform. A visual library is embedded into the Simulink browser by the aid of GUI modeling. Figure 6 shows the photograph of the wind turbine library under Simulink browser. The main advantage of using the lookup table method is that the actual data (3200 points) are stored where the model manipulates its real validity based on the real points fitting. The mathematical model could be correlated based on the actual data stored in the table model. The watt points are varying from 0.5 kW to 8000–10,000 kW according to many different manuals. The data were obtained from about 50 different companies working in the field of manufacturing of wind turbines. The data points are fitted via two methods. The first method is done by the curve fitting tool box, and the second is done by the neural network technique. The model is presented and correlated as a function of wind turbine power (*HP*, kW) according to the following equations:

The starting wind speed (m/s) as a function of turbine power (*HP* kW) is calculated as follows

$$Vw_s = 4.084 \times \epsilon^{(3.93^{-6} \times HP)} - 1.241 \times \epsilon^{(-0.0007313 \times HP)} \tag{33}$$

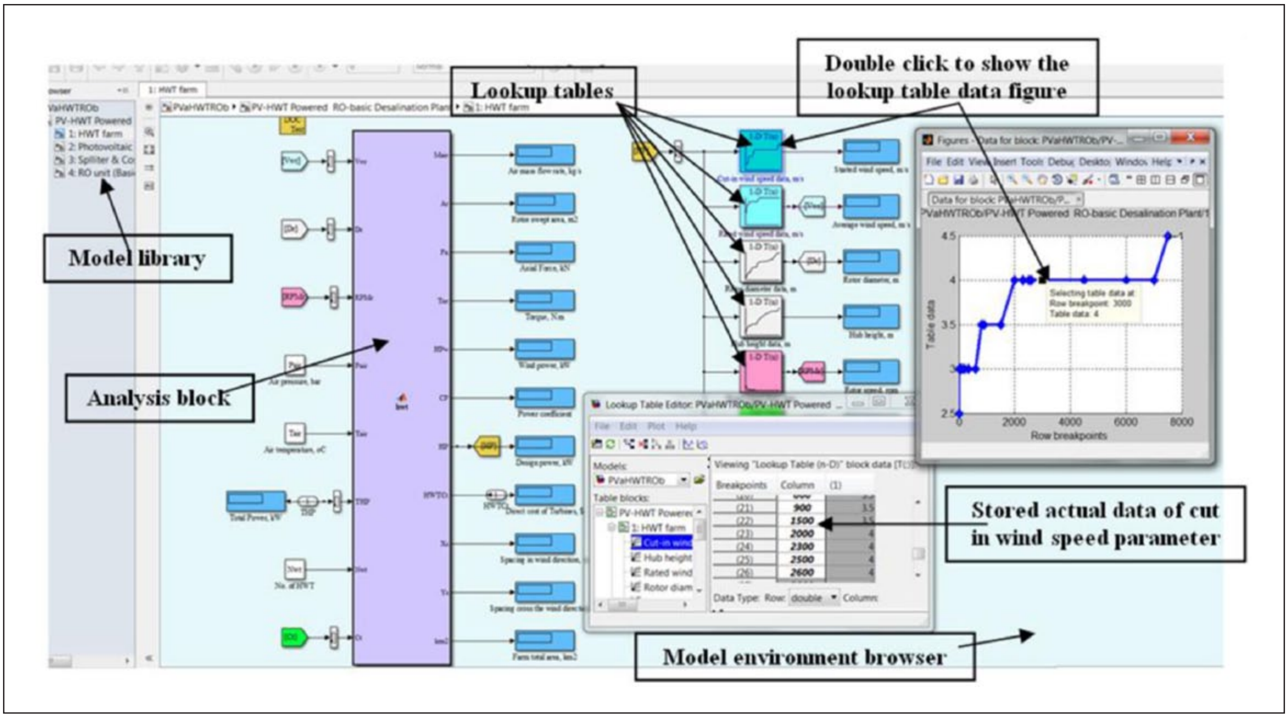

Figure 6. Look up table method for HWT model.

The average wind speed (m/s) is then calculated as

$$Vw_a = 9.378 \times (HP^{0.09862}) \tag{34}$$

The rotor diameter (m) is obtained as follows

$$Dr = 2.573 \times (HP^{0.4414}) \tag{35}$$

The tower (Hub) height (m) is calculated as follows

$$Hh = 1.437 \times (HP^{0.5046}) + 5.354 \tag{36}$$

Air density (kg/m³) is calculated based on air and pressure temperature

$$\rho_{air} = \frac{P_{air} \times 100}{0.287 \times (T_{air} + 273.15)} \tag{37}$$

where P_{air} is in bar and T_{air} is in °C.

The rotor swept area (m²) is then calculated based on the rotor diameter Dr

$$Ar = \pi \times \left(\frac{Dr}{2}\right)^2 \tag{38}$$

The air mass flow rate (kg/s) is then calculated based on the density, rotor swept area, and average wind speed

$$M_{air} = \rho_{air} \times Ar \times Vw_a \tag{39}$$

The required wind power (kW) is calculated as follows

$$HP_w = \frac{((1/2)\times \rho_{air} \times Ar \times (Vw_a{}^3)}{1000} \tag{40}$$

The power coefficient is calculated from the assigned power *HP* and the aerodynamic power *HPw*

$$CP = \frac{HP}{HP_w} \tag{41}$$

The rotor speed (r/min) is obtained as follows

$$RPM_r = 347.6 \times (HP^{-0.2909}) - 16.91 \tag{42}$$

The rotor torque (N m) based on the power of the turbine and ω is calculated as follows

$$\omega = \frac{(2\times \pi \times RPM_r)}{60} \tag{43}$$

$$Tor = \frac{(1000 \times HP)}{\omega} \tag{44}$$

The turbine unit cost ($) is calculated as follows

$$C_t = (HP \times 310.985) + 390.8 \tag{45}$$

The number of wind turbines can be calculated relating to the total demanded power (*THP* kW) from the wind farm

$$NWT = \frac{THP}{HP} \tag{46}$$

ANN method for HWT

The regression model for the HWT that performed by the ANN method is presented in this subsection. As presented earlier in PV section, the hidden layer would be nine neurons and the output layer would be six neurons. The input is one parameter (power) and the outputs are six parameters. Figure 7 shows the neural network model concept for the HWT. Figure 8 shows the model program for the HWT by the aid of ANN tool box.

The ANN regression equations are presented as follows

$$P_n = \frac{P - 753.6348}{1.6935^3} \tag{47}$$

where P_n represents the normalized input for the power and the following equations lead to the required derived equation. Equation (47) presents the normalized input for the power and the following equations lead to the required derived equation, where *n* subscript denotes normalized parameters, *EI* is the sum of input with input weight and input bias for each node in a hidden layer in a neural network, and *Fi* is the output from each node in a hidden layer to output layer according to transfer function

$$\begin{aligned} E2 &= -9.9346 \times P_n + 39.4127 \\ E3 &= 5.1501 \times P_n - 3.0470 \\ E4 &= -238.6727 \times P_n + 24.3577 \\ E5 &= -3.2422 \times P_n + 3.7053 \end{aligned} \tag{48}$$

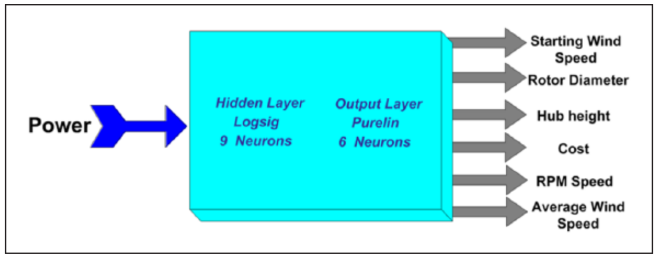

Figure 7. HWT neural network model concept.

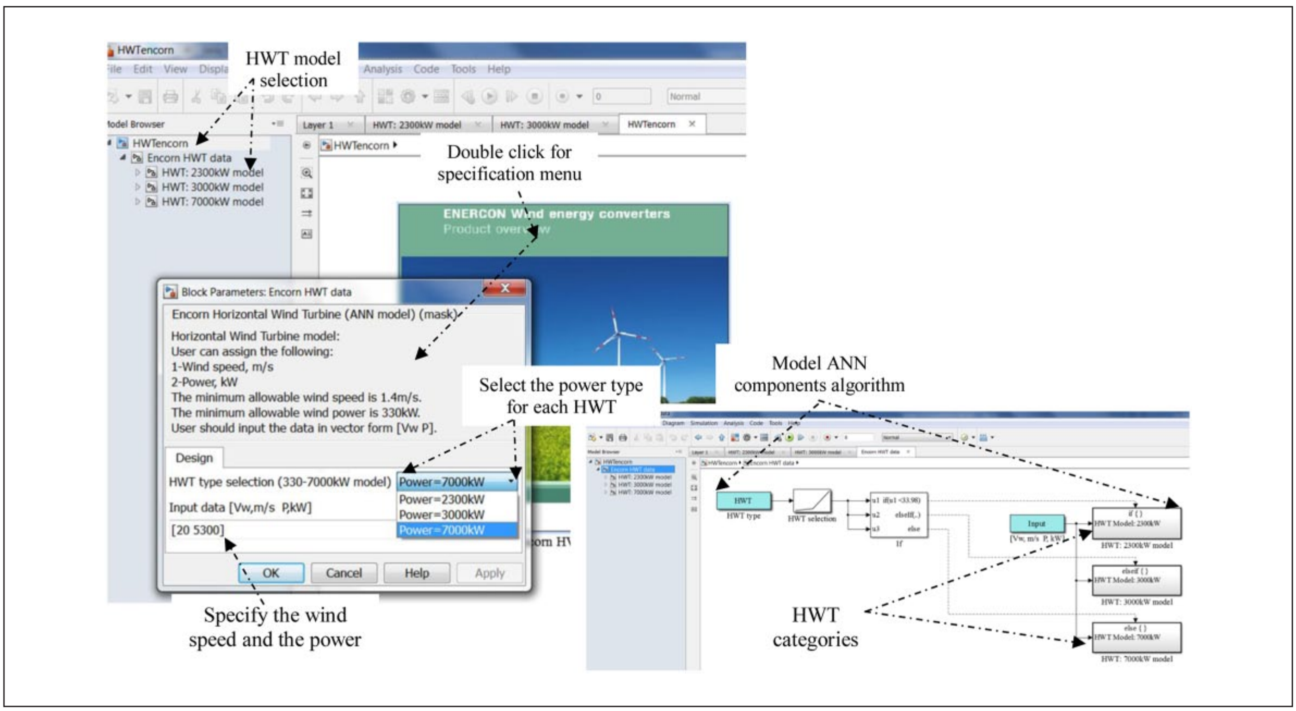

Figure 8. ANN model for HWT simulation program.

$$
\begin{aligned}
E6 &= -59.8291 \times P_n + 78.8676 \\
E7 &= -7.2582 \times P_n + 3.2749 \\
E8 &= -20.1764 \times P_n - 1.9335 \\
E9 &= 804.8057 \times P_n + 365.3206 \\
F_{1,\ldots,9} &= \frac{1}{(1+\epsilon^{-E_{1\ldots9}})}
\end{aligned}
\tag{49}
$$

The normalized starting wind speed relation from ANN is then presented in equation (50)

$$
\begin{aligned}
Vw_n = 10^3 \times [&-3.8299 \times F1 - 2.9017 \times F2 + 8.5491 \times F3 - 2.0946 \times F4 + 7.3592 \times F5 \\
&- 2.293 \times F6 + 7.2199 \times F7 - 0.0619 \times F8 + 0.4402 \times F9 - 3.8263]
\end{aligned}
\tag{50}
$$

Also, the normalized rotor diameter relation from ANN is found in equation (51)

$$
\begin{aligned}
Dr_n = 10^3 \times [&-0.0866 \times F1 + 1.1334 \times F2 - 0.4651 \times F3 - 2.7738 \times F4 - 3.2725 \times F5 \\
&+ 1.4052 \times F6 + 3.6699 \times F7 - 0.1222 \times F8 + 0.1254 \times F9 - 0.0908]
\end{aligned}
\tag{51}
$$

The hub normalized hub height by the ANN is found by equation (52)

$$Hh_n = 10^3 \times [-0.1375 \times F1 + 1.0748 \times F2 - 0.2275 \times F3 - 2.9003 \times F4 - 3.1328 \times F5 + 1.3696 \times F6 + 3.9662 \times F7 - 0.1268 \times F8 + 0.0178 \times F9 - 0.1428] \tag{52}$$

The normalized cost relation from ANN is presented in equation (53)

$$Ct_n = 10^3 \times [-0.0353 \times F1 + 0.4173 \times F2 - 0.1202 \times F3 - 1.0839 \times F4 - 1.2123 \times F5 + 0.5244 \times F6 + 1.4655 \times F7 - 0.0480 \times F8 + 0.0064 \times F9 - 0.0389] \tag{53}$$

The normalized RPM (r/min) speed relation from ANN is formulated by equation (54)

$$RPM_n = 10^3 \times [0.4985 \times F1 - 2.8698 \times F2 + 3.2212 \times F3 + 4.4604 \times F4 + 8.0036 \times F5 - 3.1991 \times F6 - 4.6696 \times F7 + 0.2045 \times F8 - 2.9357 \times F9 + 0.5314] \tag{54}$$

The normalized average wind speed is existed by equation (55)

$$Vw_{a_n} = 10^3 \times [-1.3939 \times F1 + 0.9427 \times F2 + 1.2284 \times F3 - 4.3178 \times F4 - 2.9426 \times F5 + 1.4554 \times F6 + 6.691 \times F7 - 0.1833 \times F8 + 1.143 \times F9 - 1.4083] \tag{55}$$

Then un-normalized outputs are performed as follows

$$Vw_s = 10^5 \times 0.000975 \times Vw_n + 10^5 \times 0.000098 \tag{56}$$

$$Dr = 10^5 \times 0.0004 \times Dr_n + 10^5 \times 0.0003 \tag{57}$$

$$H = 10^5 \times 0.0003 \times H_n + 10^5 \times 0.0003 \tag{58}$$

$$Ct = 10^5 \times 8.8069 \times Ct_n + 10^5 \times 4.6983 \tag{59}$$

$$RPM_r = 10^5 \times 0.0012 \times RPM_n + 10^5 \times 0.0014 \tag{60}$$

$$Vw_a = 10^5 \times 0.000049 \times Vw_{a_n} + 10^5 \times 0.0001 \tag{61}$$

The models validation

PV code models

The PV model code validation results (ANN and lookup table) are presented in this section. The ANN and lookup table data show a very good agreement corresponding to the actual data presented. Figure 9 shows the variations of open circuit voltage versus the variations of the module power. It is clear from Figure 9 that the ANN and lookup table data match with the actual data fed to the model. The model varies from 0.5 W up to 300 W. The open circuit voltage is found in the range of 20–50 Volt. Increasing the power would increase the open circuit voltage parameter. The same behavior is noticed in Figure 10. The short circuit current is increased by increasing the module power. The short circuit current was not exceeded over 8–9 A according to 300 W module. The cell efficiency parameter is very important because it could determine the number of cells fit on the module structure. The behavior of the cell efficiency and number of cell parameters is shown in Figures 11 and 12. Figure 11 indicates that the cell efficiency is varied between the range of 14%–17%. Figure 12 shows the constant line correlation corresponding to the module power. The number of cells per module is nearly

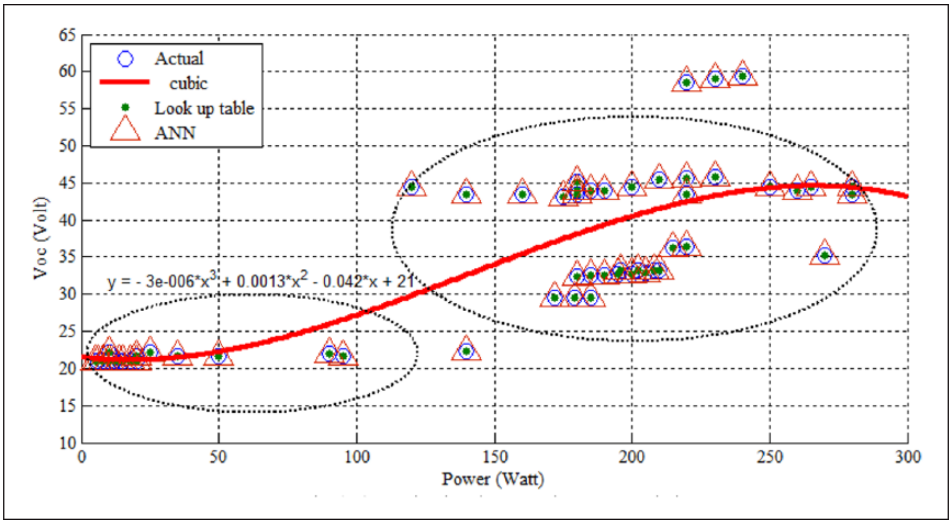

Figure 9. Open circuit voltage versus the power variations.

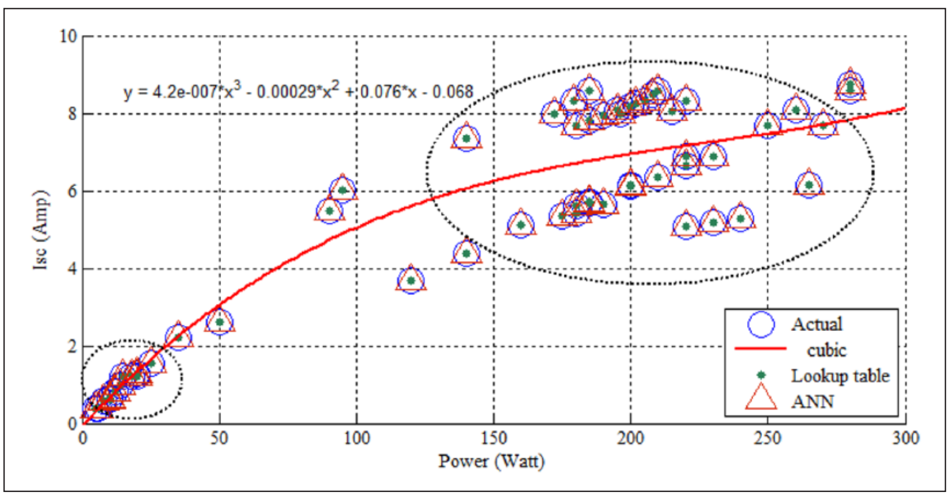

Figure 10. The variation of short circuit current versus the power variation.

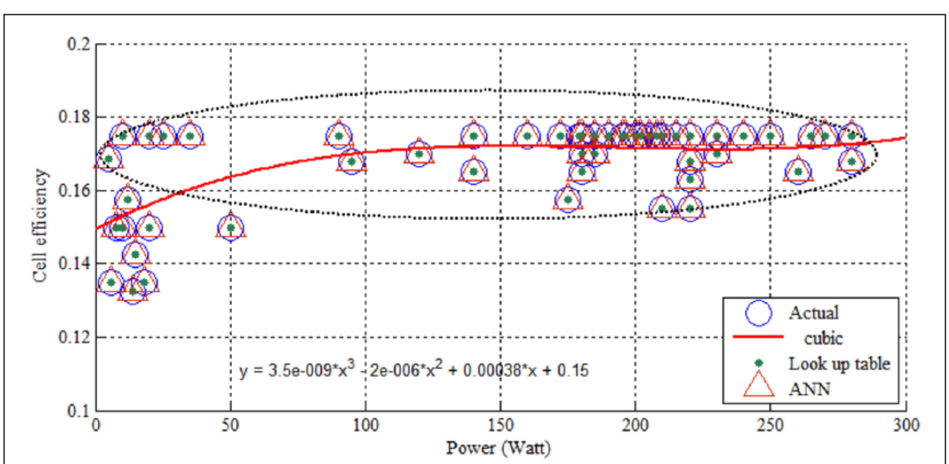

Figure 11. The PV cell efficiency versus the power variation.

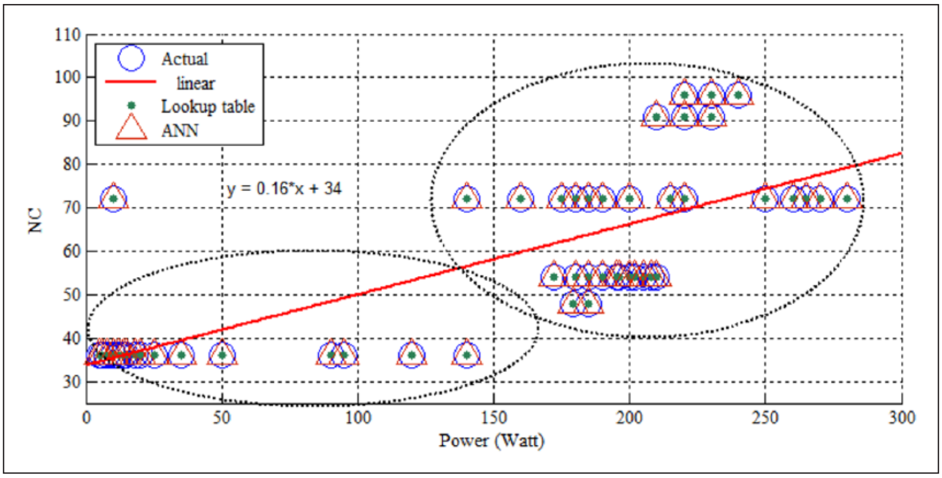

Figure 12. The number of cells parameter versus the variation of power parameter.

between 35 and 80 cells per module according to 0.5–300 W, respectively. The manufacturer deals with the number of cell parameter as a constant line because of the design limitations of the frame dimension, the structure, the weight, and the power from the module panel. The normalized data fit shows a very good agreement corresponding to the actual data. It has become easy for the users and designers to simulate and model such units or systems without being involved with any other complicated equations or complicated differential equations models. Such examples from Figures 9 to 12 represent a very good recognition to the designers to understand the PV design without any complicated calculations or extra equation with generality and simplicity corresponding to only one parameter, which is the power.

HWT models

Results for HWT type of wind turbines are shown and highlighted in this section. Figure 13(a) to (f) interprets the data results comparisons between the actual data, the polynomial correlations, and the ANN model based on starting wind speed, rotor diameter, hub height, and rotor speed and cost. It is obvious from the figure that the actual data are highly matched with the polynomial (poly) correlations and the ANN model.

In general, all addressed parameters are increased by the increase in the unit power (kW). However; the normal vice versa of the power increasing is the decreasing in the rotor speed (r/min); thence, the torque is increased with the increasing in the power. Start wind speed parameter was not exceeded over 4–4.5 m/s as a maximum value. Rated wind speed was not exceeded over 20–25 m/s. Such value is quite suitable for the unit safety.

For the power range from 1 to 1000 kW, the rotor diameter and hub height were found in the ranges of 50–60 m, respectively. For power category of 2000–4000 kW, the range of 70–80 m is considered as a remarkable result. For more than 5000 kW power, a value of 125 and 140 m is noticed for rotor diameter and hub height, respectively. The cost is normally increased with the addition of the power demanded. It is found that the cost varied from 1000$ to 4e+6$ for a power range from 0.5 to 8000 kW.

It becomes very easy for the designer to choose the operating point based on the demanded load. The normal scenario for any designer that the required power is known; therefore, the minimum wind speed or even the rotor speed becomes very easy to be calculated, thence the category of the wind turbine. The meteorological data would play as an important parameter side by side with the selected power.

From the above correlations and figures, if we have the wind speed of the location, we can simply specify the suitable wind turbine for this location. So, this study presents a helpful simple tool for investigators, designers and customs choose a best suitable wind turbine based on wind velocity and power load. There is no need to apply the complicated aerodynamic design correlations to select the optimized operating conditions.

Results and comments (case studies)

HWT case study

As a case study of wind farm *Zafarana-5* (Abul Wafa, 2011), the demanded total power was in the range of 85 MW. The number of wind turbines was about 100 times of 850 kWe per unit. By the use of the developed models in this work, it

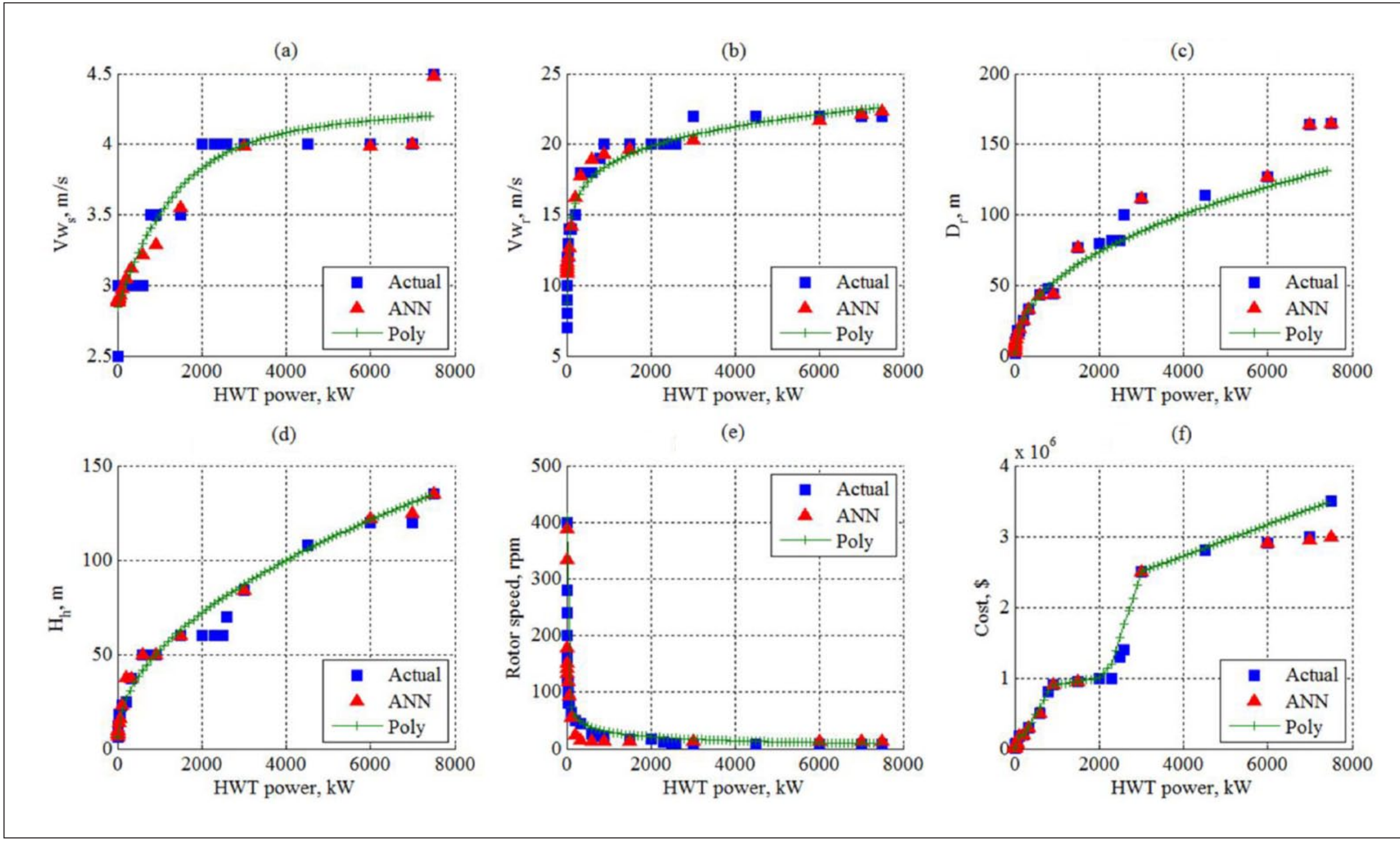

Figure 13. Data results for the HWT based on the unit power variation: (a) start wind speed, (b) rated wind speed, (c) rotor diameter, (d) hub height, (e) rotor speed, and (f) HWT unit cost.

Table 2. Specifications and comparison results of the developed model (http://www.enercon.de/de-de/) and Zafarana-5.

Zafarana-5 (GAMESA G52)	The developed model
Rotor	Rotor
Diameter: 52 m	Diameter: 50.52 m
Swept area: 2214 m^2	Swept area: 2004 m^2
Rotational speed: 19.44–30.8 r/min	Rotational speed: 31.95 r/min
Blades	Blades
Number of blades: 3	Number of blades: 3
Tower	Tower
Type modular height: 44, 55, and 65 m	Type modular height: 48.57 m
Model results	
Mass flow rate (kg/s)	4.466e+4
Start wind speed (m/s)	12.87
Rated wind speed (m/s)	18.24
Axial force on the turbine wheel (kN)	362
Power coefficient	0.1144

becomes very easy to specify the input (power = 850 kWe/unit) to get the important specs of the turbine unit. Therefore, the designers and/or the Egyptian government would become able to put in mind the wind farm dimensions before the establishment operations.

It is found by Emami and Noghreh (2010) that the optimum spacing in a row is 8–12 times the rotor diameter in the wind direction and 1.5–3 times the rotor diameter in the cross-wind direction. Therefore, in this case study, the spacing in wind direction would become 606.3 m in wind direction and 151.6 m crosswind direction. Thence, the region of four turbines would become 0.092 km^2. Table 3 shows the data results comparison of the developed model in this work and the data obtained from *Zafarana-5* (Abul Wafa, 2011) wind farm. Table 2 shows that there is a very good matching between the simulated data and the real data from *Zafarana-5*.

To better understand the effect of HWT power and operating wind speed, a GUI model is used. Using the neural network technique in implementing a neural model to connect between the variables that entering the rated power, V_w and power ranges as inputs to generate CP, D_r, H_h, and RPM. This is done to make benefits from the ability of the neural network of interpolation between points and also curves.

The algebraic equations are deduced to use it without training the neural unit in each time. This model delivers a suitable number of layers and neurons in each stratum. Some of training data are well depicted in the following three-dimensional (3D) figures for all inputs and targets (outputs). Figure 14 shows the effect of V_w and design power parameters on the actual power. The figure shows that at 15 m/s the curve remains constant till 25 m/s. Therefore, it depends on the designer to select the operating power according to wind map of the location of the procedure. It is obvious that the rotor diameter and hub height parameters give the potential outcome in the face of the same wind speed. Figure 15 shows the effect on the power coefficient parameter. It is pinpointed on the 3D curve that the maximum turbine efficiency is located between 10 and 15 m/s on rated wind speed. Increasing the rated wind speed over 15 m/s would decrease the HWT efficiency. Furthermore; the efficiency was not exceeding over 0.45–0.48 as a target value.

Figure 16 shows the behavior of the rotor diameter based on the wind velocity and power parameters. As expected, the rotor diameter is considered an important role that is affected by the power produced. Increasing the rotor diameter would increase the power, kW. It is very important for the designers that in case of electing a category range of high power, the rotor diameter would be high. Meanwhile, increasing the diameter would increase the costs of the HWT. Figure 17 shows the effect of wind speed and rated power parameters on the hub height. As it is expected, the hub height is increased by the increase rated power at the same wind speed.

Figure 18 shows the behavior of the rotor speed parameter according to each power category. It is noticed on the figure that increasing the wind speed would increase the RPM. However; in general, increasing the power (according to each category, that is, 300 or 1000 kW) would decrease the RPM due to many reasons such as the hub height and the rotor diameter that is, large sizes and extra weight. It is obvious in Figure 18 that the effect of wind speed on the rotor speed is highly noticed.

PV case study

The officials of the Suez Bakery foundation, Suez-Egypt, decided to power on a huge bakery foundation established on 1000 m^2 area by the off-grid PV solar power. The bakery consumes about 30–45 kWh. The developed code is utilized to

Table 3. Specifications and comparison results of the developed model and reference (www.dpl-energy.com) based on Suez Bakery Foundation case study.

Operating conditions (known parameters)	
1. Solar radiation (W/m^2): 550 (Nafey et al., 2010)	
2. Ambient temperature (°C): 25	
3. Clearness index: 0.6	
4. Number of cloudy days: 2	
Characteristics (known parameters)	
1. PV type: mono-crystalline	
2. Maximum power per module: 250 Wp	
3. Total demanded power (kW): 45	
4. Battery bank voltage/battery voltage (V): 220/2	
5. Battery efficiency: 0.85–0.9	
Target results (unknown parameters)	
dpl-energy (www.dpl-energy.com)	The developed code
1. Maximum power/module (W): 250	1. Maximum power/module (W): 250
2. Open circuit voltage (V): 44.4	2. Open circuit voltage (V): 47.2
3. Short circuit current (A): 7.656	3. Short circuit current (A): 7.8
4. Cell efficiency (%): 17.5	4. Cell efficiency (%): 17.5
5. Module efficiency (%): 13.5	5. Module efficiency (%): 14.2
6. Number of cells: 72	6. Number of cells: 72
7. Net weight (kg): 23	7. Net weight (kg): 23
8. Total system area (m^2): 510	8. Module dimension (m^3): 0.095
9. Number of batteries: 110	9. Number of modules: 180
	10. Module area (m^2): 2.942
	11. Total system area (m^2): 529
	12. Number of batteries: 110
	13. PV costs (based on 1\$/W), \$: 6.94e+4\$

PV: photovoltaic.

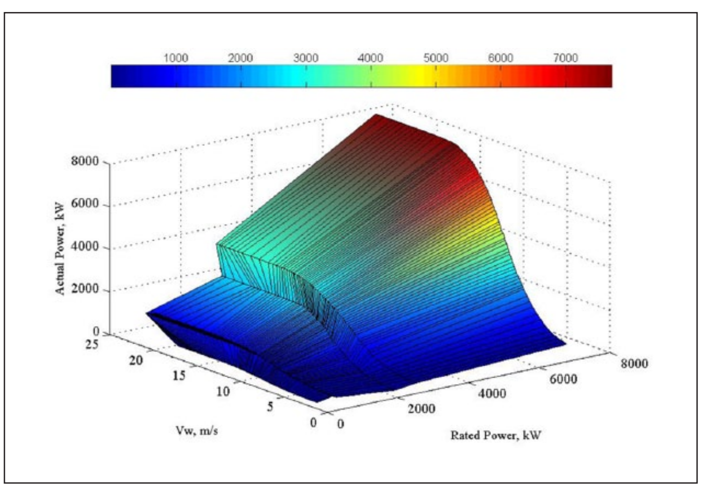

Figure 14. The effect of wind speed (m/s) and rated power on the demanded actual power (kW).

calculate the required important data for the bakery foundation. The officials wanted to know some important parameters such as the required area, and the total cost (purchase, installation, batteries, cables, structure, etc.). Table 3 summarizes the input parameters required for the code, the calculated analysis, and the validity of the code when comparing with the calculated analysis from PV energy company (www.dpl-energy.com). It is obvious that the calculated data from the developed code are favorably matched with the analysis presented by the PV energy company. The operating conditions are calculated according to solar radiation and meteorological data due in the spring season to ensure continuous and less uncertainty of the power during winter time. Maximum power per module is 250 W, with cell efficiency of 17.5%, 72

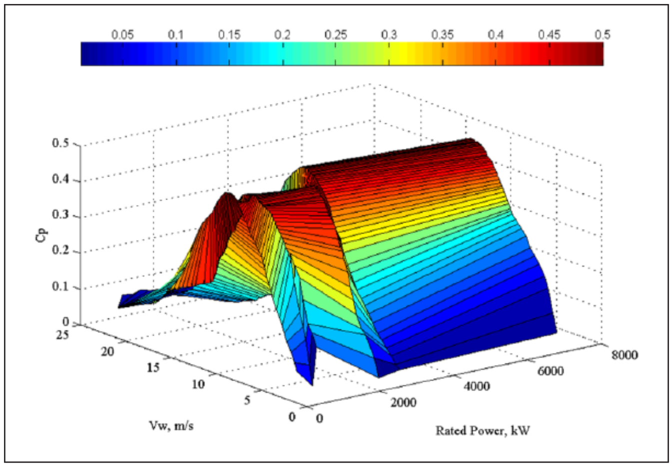

Figure 15. The effect of wind speed (m/s) and rated power (kW) on the power coefficient of the HWT.

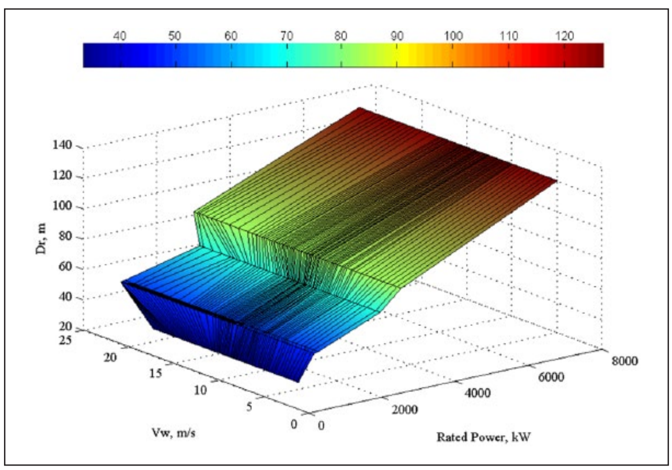

Figure 16. The effect of wind speed (m/s) and rated power on the rotor diameter (m).

cells, and 180 modules. The 45-kW load would harvest about 530 m^2 with battery bank equal to 110 batteries. The system cost would be in the range of 6.94e+4$ including the structure, cables, and inverter.

It is obvious from the previous case studies that it is become very easy to the investor/designer to specify the domain area or the location of the operation based on the results obtained. Furthermore; the developed models (ANN or polynomial via GUI) have many features such as:

- Easy modeling manipulation: User can easily copy and paste the equations then obtain the results.
- The model is so accurate enough to cover a wide range of power as presented (0.5–8000 kW for HWT).
- The developed models are built based on the real data from manufacturing manuals for wind turbines and PV performance sheets.
- The developed model is then being ready to be combined with other technologies or units as a hybrid system such as desalination, or auxiliary power generation, or PV technologies.
- The designer has a great ability to assign the number of wind turbines and/or PV systems that could be used in the wind or solar farms based on the unifying power and the total power.
- GUI model based ANN tool box is examined in the HWT case showing that the rotor diameter and hub height parameters are considered the main reasons to increase the power demanded by the HWT.

Conclusion

The modeling technique and the proposed circuit model are useful for power electronics designers who need a simple, fast, accurate, and easy-to-use modeling method for using in simulations of PV and HWT systems. Traditional modeling

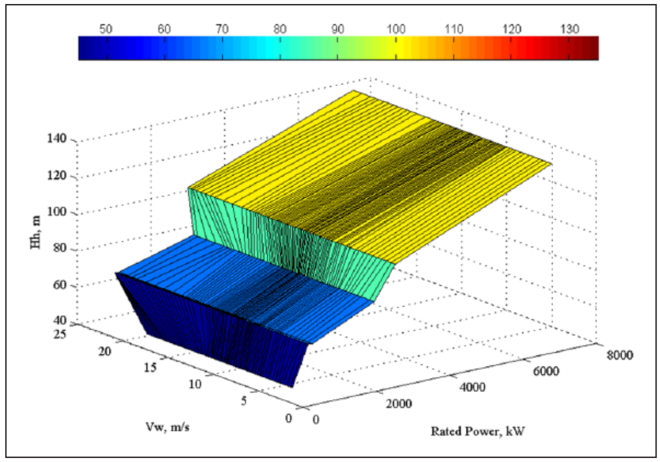

Figure 17. The effect of wind speed (m/s) and rated power on the hub height (m).

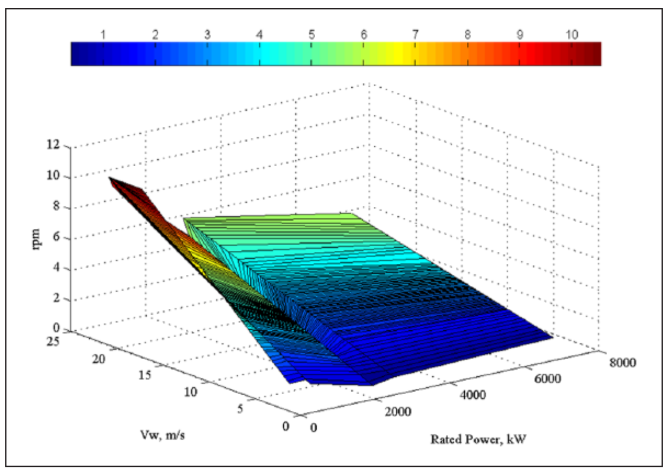

Figure 18. The effect of wind speed (m/s) and rated power on the RPM.

techniques are too difficult for the investor/designer to specify accurately the specific point of design (power, module efficiency, wind speed, design limits, etc.). Thence, the need for an accurate software programming to make a general selection based design and simulation of different types of wind turbines and PV system is essential. Therefore, two techniques of modeling (GUI with lookup table and ANN) are used in this work to design and simulate PV systems and HWT.

The neural network units are implemented, using the back-propagation learning algorithm due to its benefits to have the ability to predict values in-between learning values, also make interpolation between learning curve data. This is done with suitable number of network layers and neurons at minimum error and precise manner. The ANN regression function for each unit is introduced to be used directly without operating the neural model each time. The required models are investigated and compared with the actual data from the manufacturer's manuals of the PV and wind turbines. Results reveal that the actual data are matched well with the developed model results. The models have many features such as the following:

- Easy model construction.
- Covering a wide range of power.
- Easy of combination with other technologies such as desalination and/or PV.
- Ease of converting the model codes into C++ or Visual Basic software programming.
- It becomes very easy for the designer to specify the power point and simply elect the turbine from the market based on the model data results.
- The developed model is very easy to be used instead of using the complicated aerodynamic equations of the wind turbines and complicated correlations for the PV systems. No need for complicated differential equations and correlations.
- Only one parameter is needed to be assigned (power load) to solve the model outputs.

Declaration of conflicting interests

The author(s) declared no potential conflicts of interest with respect to the research, authorship, and/or publication of this article.

Funding

The author(s) received no financial support for the research, authorship, and/or publication of this article.

References

Abidin Firatoglu Z and Yesilata B (2004) New approaches on the optimization of directly coupled PV pumping systems. *Solar Energy* 77: 81–93.

Abul Wafa AR (2011) Matching wind turbine generators with wind regime in Egypt. *Electric Power Systems Research* 81: 894–898.

Ahmad GE and Schmid J (2002) Feasibility study of brackish water desalination in the Egyptian deserts and rural regions using PV systems. *Energy Conversion and Management* 43: 2641–2649.

Ammar MB, Chaabene M and Chtourou Z (2013) Artificial neural network based control for PV/T panel to track optimum thermal and electrical power. *Energy Conversion and Management* 65: 372–380.

Ashhab MSS (2008) Optimization and modeling of a photovoltaic solar integrated system by neural networks. *Energy Conversion and Management* 49: 3349–3355.

Badescu V (2006) Simple optimization procedure for silicon-based solar cell interconnection in a series–parallel PV module. *Energy Conversion and Management* 47: 1146–1158.

Bououden S, Chadli M, Filali S, et al. (2012) Fuzzy model based multivariable predictive control of a variable speed wind turbine: LMI approach. *Renewable Energy* 37: 434–439.

Burgelman M, Verschraegen J, Degrave S, et al. (2004) Modeling thin-film PV devices. *Progress in Photovoltaics: Research and Applications* 12: 143–153.

Chenni R, Makhlouf M, Kerbache T, et al. (2007) A detailed modeling method for photovoltaic cells. *Energy* 32: 1724–1730.

De Soto W, Klein SA and Beckman WA (2006) Improvement and validation of a model for photovoltaic array performance. *Solar Energy* 80: 78–88.

Emami A and Noghreh P (2010) New approach on optimization in placement of wind turbines within wind farm by genetic algorithms. *Renewable Energy* 35: 1559–1564.

Ghoneim AA, Al-Hasan AY and Abdullah AH (2002) Economic analysis of photovoltaic-powered solar domestic hot water systems in Kuwait. *Renewable Energy* 25: 81–100.

Hansen MOL, Sorensen JN, Voutsinasb S, et al. (2006) State of the art in wind turbine aerodynamics and aero-elasticity. *Progress in Aerospace Sciences* 42: 285–330.

Hasnain SM and Alajlan SA (1998) Coupling of PV-powered RO brackish water desalination plant with solar stills. *Desalination* 116: 57–64.

Ismail MS, Moghavvemi M and Mahlia TMI (2013) Design of an optimized photovoltaic and microturbine hybrid power system for a remote small community: Case study of Palestine. *Energy Conversion and Management* 75: 271–281.

Jafarian M and Ranjbar AM (2010) Fuzzy modeling techniques and artificial neural networks to estimate annual energy output of a wind turbine. *Renewable Energy* 35: 2008–2014.

Janajreh I, Qudaih R, Talab I, et al. (2010) Aerodynamic flow simulation of wind turbine: Downwind versus upwind configuration. *Energy Conversion and Management* 51: 1656–1663.

Kim JP, Lim H, Song JH, et al. (2011) Numerical analysis on the thermal characteristics of photovoltaic module with ambient temperature variation. *Solar Energy Materials & Solar Cells* 95: 404–407.

Kurtz S, Whitfield K, Tamizhmani G, et al. (2011) Evaluation of high-temperature exposure of photovoltaic modules. *Progress in Photovoltaics: Research and Applications* 19: 954–965.

Kusiak A and Song Z (2010) Design of wind farm layout for maximum wind energy capture. *Renewable Energy* 35: 685–694.

Lo Brano V, Orioli A, Ciulla G, et al. (2010) An improved five-parameter model for photovoltaic modules. *Solar Energy Materials & Solar Cells* 94: 1358–1370.

Mellit A and Pavan AM (2010) Performance prediction of 20kW grid-connected photovoltaic plant at Trieste (Italy) using artificial neural network. *Energy Conversion and Management* 51: 2431–2441.

Nafey AS, Sharaf MA and García-Rodríguez L (2010) A new visual library for design and simulation of solar desalination systems (SDS). *Desalination* 259: 197–207.

Parida B, Iniyan S and Goic R (2011) A review of solar photovoltaic technologies. *Renewable and Sustainable Energy Reviews* 15: 1625–1636.

Sandrolini L, Artioli M and Reggiani U (2010) Numerical method for the extraction of photovoltaic module double-diode model parameters through cluster analysis. *Applied Energy* 87: 442–451.

Thapar V, Agnihotri G and Sethi VK (2011) Critical analysis of methods for mathematical modeling of wind turbines. *Renewable Energy* 36: 3166–3177.

Vazquez M and Rey-Stolle I (2008) Photovoltaic module reliability model based on field degradation studies. *Progress in Photovoltaics: Research and Applications* 16: 419–433.

Villalva MG, Gazoli JR and Filho ER (2009) Comprehensive approach to modeling and simulation of photovoltaic arrays. *IEEE Transactions on Power Electronics* 24(5): 1198–1208.

Zhang L and Bai YF (2005) Genetic algorithm-trained radial basis function neural networks for modeling photovoltaic panels. *Engineering Applications of Artificial Intelligence* 18: 833–844.

Zouari A and Arab AB (2011) Effect of the front surface field on crystalline silicon solar cell efficiency. *Renewable Energy* 36: 1663–1670.

Appendix 1

Notation

A	area (m^2)
Ar	rotor swept area (m^2)
Ct	turbine cost for HWT case ($)
CP	power coefficient (%)
Dr	rotor diameter (m)
Ei	ANN parameter
Fi	ANN parameter
Hh	hub height (m)
HP	power (kW)
HPw	wind power (kW)
I_{sc}	short circuit current (A)
M_{air}	air mass flow rate (kg/s)
NC	number of cells
P	power (kW)
Pn	normalized power by ANN (kW)
Tor	torque (N m)
V	velocity (m/s)
Vw_s	starting wind speed (m/s)
Vw_a	average wind speed (m/s)
V_{oc}	open circuit voltage (V)
ρ_{air}	density (kg/m^3)
ω	angular velocity (Omega) (rad/s)

Subscripts

air	air
a	average
b	battery
i	number
h	height
m	module
n	normalized
r	rotor
s	start
t	total
w	wind